ELSEVIER

Coordination Chemistry Reviews
216–217 (2001) 127–154

COORDINATION CHEMISTRY REVIEWS

www.elsevier.com/locate/ccr

Control of photoinduced energy transfer between metal-polypyridyl luminophores across rigid covalent, flexible covalent, or hydrogen-bonded bridges

Michael D. Ward [a,*], Francesco Barigelletti [b]

[a] *School of Chemistry, University of Bristol, Cantock's Close, Bristol BS8 1TS, UK*
[b] *Istituto FRAE-CNR, Via P. Gobetti 101, 40129 Bologna, Italy*

Received 8 August 2000; accepted 17 November 2000

Contents

* Corresponding author. Tel.: +44-117-9287655; fax: +44-117-9290509.
E-mail address: mike.ward@bristol.ac.uk (M.D. Ward).

PII: S0010-8545(00)00409-4

Abstract

This review describes four recent examples of how photoinduced energy-transfer in dinuclear complexes can be manipulated or controlled according to the nature of the bridging pathway between the metal-polypyridyl luminophores. In the first examples, the interacting fragments [polypyridyl complexes of Ru(II), Os(II) or Re(I)] are covalently linked by the bridging ligand 2,2′:3′,2″:6″,2‴-quaterpyridine which has two inequivalent bipyridyl binding sites in close proximity. In heterodinuclear Ru–Os and Ru–Re complexes, efficient inter-component photoinduced energy-transfer occurs, with the emission characteristics being sensitive to the electronic difference between the two bipyridyl sites. This, in the Ru–Re diads either Ru→Re or Re→Ru energy transfer can occur depending on which metal fragment is in which binding site. The second example is of a supramolecular assembly in which the interacting Ru(II) and Os(II) mononuclear components are associated in CH_2Cl_2 solution via a reversible hydrogen-bonding interaction between peripheral nucleobase groups. Watson–Crick base-pair formation results in a Ru–Os diad showing efficient Ru→Os energy-transfer across the hydrogen-bonded interface. The third example describes a Ru–Re diad in which the flexible bridging ligand incorporates a diazacrown macrocyclic unit. Binding of Ba^{2+} into this macrocycle at 77 K results in a decrease in the rate of Re→Ru photoinduced energy-transfer by a factor of 30, probably because of a conformational change which causes the Ru and Re components to move further apart. The final example is of a Ru–Os diad in which the $[Ru(bipy)_3]^{2+}$ and $[Os(bipy)_3]^{2+}$ components are separated by a flexible poly(oxoethylene) 18-atom chain whose conformation is solvent dependent. Changing the solvent polarity results in a conformational change in the chain, and consequently a change in the Ru···Os separation and hence the Ru→Os energy-transfer rate. Thus, the long-range energy-transfer interaction can be controlled by the polarity of the solvent.

Keywords: Photoinduced energy-transfer; Ruthenium; Osmium; Rhenium; Polypyridyl complexes; Hydrogen-bonding; Azacrown macrocycles; Conformational change; Molecular switches; Luminescence

1. Introduction

The study of photoinduced energy or electron transfer between a chromophore and a quencher in polynuclear complexes, one of the most intensively studied areas in current inorganic chemistry, is of interest for two distinct reasons. The first is the desire to understand and mimic the naturally occurring process of photosynthesis, which relies on a complex series of energy-transfer and electron-transfer processes to harness the energy of sunlight by converting CO_2 and water to sugars. The second is to exploit these processes in artificial systems, in ways that have not developed naturally, for applications as diverse as molecular sensing, photocatalysis, and molecular electronics.

To prepare chromophore–quencher assemblies for such studies requires a suitable way to hold the two components close enough together that they can interact effectively. Commonly, this is to use a bridging ligand in which there is a covalent linkage between the two sites; there are very many such covalently-linked systems, of which the commonest are based on metalloporphyrins or polypyridyl complexes of d^6 metals [Ru(II), Os(II), Re(I)] [1–5]. Alternatively, non-covalent interactions such as hydrogen-bonding or aromatic π-stacking (or often a combination of several such interactions) can be used to control association of the chromophore and quencher, following the 'supramolecular' methods that are employed in natural photosynthesis [6]. In either case, the bridging ligand has two roles: a structural one (to hold the component parts together at a particular distance and orientation), and an electronic one (to assist in mediation of inter-component interactions that occur via a through-bond pathway). It will be obvious that the way the components are linked together will profoundly affect the structures and photophysical properties of polynuclear complexes.

In this article are described four recent examples from our laboratory of how photoinduced energy transfer from a chromophore to a quencher can be controlled — switched, to some extent — by exploiting the properties of the bridging pathway between the metal centres. Whilst photoinduced energy-transfer is now well known, the ability to switch on or off the metal-to-metal communication by some external stimulus has not been addressed so much, and has clear relevance to the development of photonic (as opposed to electronic) devices and sensors.

2. Photoinduced energy-transfer in Ru–Os and Ru–Re covalently-linked polynuclear assemblies

2.1. Synthesis of the bridging ligand 2,2′:3′,2″:6″,2‴-quaterpyridine and the structures of its complexes

The bridging bis-bidentate ligand 2,2′:3′,2″:6″,2‴-quaterpyridine was unexpectedly prepared by reductive coupling of 2,2′-bipyridine with LDA (Scheme 1) [7,8]. Whereas pyridine under the same conditions ultimately yields 4,4′-bipyridine via a symmetric coupling of two pyridine radical anions [9], and other bipyridines likewise dimerise at the C^2 or C^4 positions [10], we believe that reaction of 2,2′-bipyridine with LDA follows a different course in which metalled 3-lithio-2,2′-bipyridine — stabilised by intramolecular chelation by the second pyridyl ring — performs a nucleophilic attack at the C^6 position of another molecule of 2,2′-bipyridine to give the non-symmetric product with a C^3–C^6 linkage between two bipyridyl fragments. We abbreviate this ligand as AB to denote the two inequivalent coordination sites, of which site A is clearly less hindered, and site B — with a bulky substituent adjacent to the metal binding site — is more hindered.

The inequivalence of the two coordination sites of AB could be exploited in preparing metal complexes. Reaction with one equivalent of a metal salt results

exclusively in coordination of the metal ion (M) to site A, leaving site B vacant; there is no statistical mixture of free ligand, mononuclear complex, and dinuclear complex which normally occurs with symmetrical ligands. Reaction of this mononuclear complex (denoted M–AB) with a second metal salt (M′) must then result in coordination at site B, to give M–AB–M′. Reversal of the sequence of addition of metal ions allows specific preparation of the positional isomer M′–AB–M, which can have different electrochemical and photophysical properties from M–AB–M′ because of the inequivalence of the two binding sites. In this way a variety of dinuclear complexes has been prepared, of which the isomeric pairs $[(bipy)_2Ru(AB)Os(bipy)_2]^{4+}$–$[(bipy)_2Os(AB)Ru(bipy)_2]^{4+}$ [Ru–AB–Os and Os–AB–Ru] [11] and $[(bipy)_2Ru(AB)Re(bipy)(CO)_3Cl]^{2+}$–$[Cl(CO)_3Re(AB)Ru(bipy)_2]^{2+}$ [Ru–AB–Re and Re–AB–Ru] [12] are discussed here. The former pair contains $\{Ru(bipy)_3\}^{2+}$ and $\{Os(bipy)_3\}^{2+}$ chromophores linked together; the latter contains $\{Ru(bipy)_3\}^{2+}$ and $\{Re(bipy)(CO)_3Cl\}$ chromophores linked together.

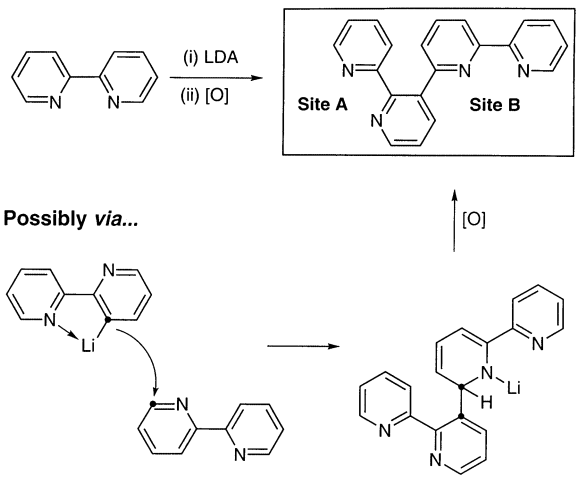

Scheme 1. Preparation of the non-symmetrical quaterpyridine ligand AB, with a tentative mechanism.

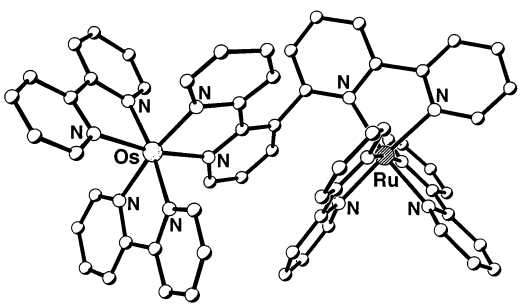

Fig. 1. Crystal structure of the complex cation of Os–AB–Ru.

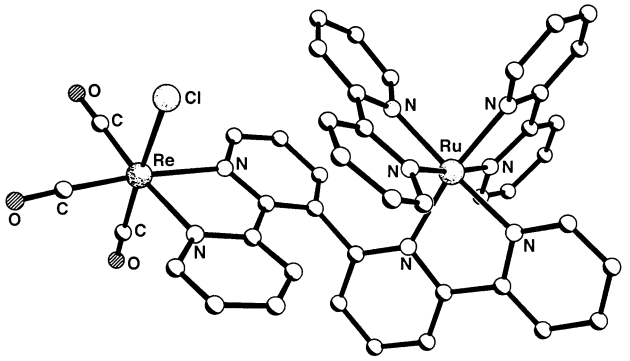

Fig. 2. Crystal structure of the complex cation of Re–AB–Ru.

Crystal structures of Os–AB–Ru and Re–AB–Ru are shown in Figs. 1 and 2, respectively, and show some points of interest. Firstly, the metal fragment at site A is relatively unhindered in every case and has a normal coordination geometry similar to those found for unsubstituted bipy complexes. In contrast the metal fragment at site B in every case is distorted by the sterically bulky substituent adjacent to the N donor of ring III, and this can be seen specifically in the lengthening of the most-hindered M–N(pyridyl) bond at the inner site B of the complex. For example in Re–AB–Ru the Ru–N(31) bond length of 2.135(6) Å is much longer than the other five Ru–N bonds, which are all close to the normal value of 2.056 Å found for $[Ru(bipy)_3]^{2+}$. Secondly, the bridging ligand has a near-perpendicular twist between the two halves, which is clearly necessary on steric grounds. Thirdly, only one diastereoisomer was observed in each case despite the presence of several chiral centres in the complexes which might have been expected to give a mixture of diastereoisomers. For Os–AB–Ru and Re–AB–Ru both metal centres are chiral, and in addition the bridging ligand is chiral by virtue of the twist between the two bipy fragments, so there are three chiral centres; however, they are not independent of one another. Given a particular configuration for the Ru tris-chelate fragment at site B, only one conformation of the bridging ligand results in favourable inter-ligand π-stacking interactions between AB and one of the bipy ligands. The configurations of the second chiral centre likewise follows from the configuration of the first two, for the same reasons: one diastereoisomer appears to be sterically preferred because of favourable inter-ligand π-stacking interactions. These dinuclear complexes may be considered as short fragments of a one-dimensional helical chain, with the helical twist arising from the angular displacement between the two halves of the bridging ligand.

2.2. Electrochemical properties of the dinuclear complexes

Electrochemical data, based on a combination of cyclic and square-wave voltammetry, is collected in Table 1 (together with data for some mononuclear reference complexes). In general, the electrochemical processes are readily to assigned as

Table 1
Summary of electrochemical and photophysical data for the complexes of 2,2′:3′,2″:6″,2‴-quaterpyridine (AB), and for the hydrogen-bonding complexes

Complex	Metal-centred redox potentials (V) [a]	Emission at room temperature			Emission at 77 K		Emission source
		λ_{max} (nm)	τ (ns)	Φ	λ_{max} (nm)	τ (μs)	
Ru–AB	+0.90	666 [b]	191	1.5×10^{-2}	588 [c]	5.9	Ru
Os–AB	+0.47	792 [b]	30	1.0×10^{-3}	722 [c]	1.3	Os
Re–AB	+0.98 [e]	626 [d]	11	9.2×10^{-4}	535 [d]	3.2	Re
Ru–AB–Os	+0.60, +1.05	756 [b]	41	3.2×10^{-3}	716 [c]	1.5	Os
Os–AB–Ru	+0.57, +1.09	808 [b]	26	1.3×10^{-3}	756 [c]	1.0	Os
Ru–AB–Re	+0.93, +1.17 [e]	644 [d]	410	2.8×10^{-2}	607 [d]	4.7	Ru
Re–AB–Ru	+1.04 [e,f]	623 [d]	23	1.4×10^{-3}	590 [d]	5.8	Re at RT; Ru at 77 K
Ru–A	+0.90	626 [g]	500	4.8×10^{-2}			
Os–T	+0.47	750 [g]	35	2.9×10^{-3}			
Ru–C	+0.90	626 [g]	350	3.6×10^{-2}			
Os–G	+0.47	744 [g]	44	2.9×10^{-3}			

[a] Measured in MeCN containing 0.1–0.2 M Bu_4NPF_6 as base electrolyte. Potentials are quoted as V vs. internal ferrocene/ferrocenium. All processes are chemically reversible except where indicated otherwise (see note e).
[b] MeCN solvent, air-equilibrated.
[c] Butyronitrile solvent.
[d] Mixed DMF–CH_2Cl_2 (9:1) solvent, air equlibrated for room temperature spectra.
[e] Irreversible Re(I)/Re(II) couple.
[f] Two processes [Ru(II)/Ru(III), and Re(I)/Re(II)] overlapping.
[g] Air-equilibrated CH_2Cl_2 as solvent.

either ligand-based reductions, or as oxidations of the various metal fragments at potentials characteristic of the well-known mononuclear analogues $[Ru(bipy)_3]^{2+}$, $[Os(bipy)_3]^{2+}$ and $[Re(bipy)(CO)_3Cl]$. On closer inspection however, the effects of the asymmetry of the bridging ligand become apparent, in that the redox potential of a metal fragment coordinated at site A is different from that of the same metal fragment coordinated at site B. The comparison of isomeric pairs of dinuclear complexes in this way ensures that any effects such as metal–metal electronic interactions which will influence the redox potentials are about the same in both isomers and therefore cancel out.

For example in Ru–AB–Os the Os(II)/Os(III) and Ru(II)/Ru(III) couples are at $+0.60$ and $+1.05$ V, respectively, such that the Os(II) centre oxidises much more easily than the Ru(II) centre. In the positional isomer Os–AB–Ru the Os(II)/Os(III) couple shifts to the lower potential of $+0.57$ V, in accordance with its move to site A, whereas the Ru(II)/Ru(III) couple shifts to the more positive potential of $+1.09$ V, in accordance with its move to site B [11]. The separation between the two couples has therefore increased from 450 to 520 mV, but the Os(II) site will still be the first to oxidise. Likewise all other relevant features of the complex (e.g. that the Os-based MLCT excited state is lower in energy than the Ru-based MLCT excited state; see later) remain basically the same, because the perturbation arising from the inequivalence of sites A and B is much less than the fundamentally large difference between the redox and photophysical properties of Ru(II) and Os(II).

However in the pair Ru–AB–Re and Re–AB–Ru, this effect is more significant, because the redox (and photophysical) properties of the component chromophores are much more similar to one another to start with [12]. Thus in Ru–AB–Re the Ru(II)/Ru(III) couple is 240 mV less positive than the Re(I)/Re(II) couple, such that the Ru(II) centre will clearly oxidise first. In Re–AB–Ru however the positive shift of the Ru(II)/Ru(III) couple and the negative shift of the Re(I)/Re(II) couple compared to Ru–AB–Re mean that the two processes are indistinguishable by voltammetry because they are essentially coincident. The redox properties of Ru–AB–Re are therefore fundamentally different from those of Re–AB–Ru, because the perturbation arising from the inequivalence of sites A and B is comparable to the difference in energies between the redox and photophysical properties of the two sites. This has important consequences for the photophysical properties of this pair of isomers.

2.3. Luminescence properties of the dinuclear complexes

Both Ru–AB–Os and Os–AB–Ru show only Os-centred emission, whatever the excitation wavelength (Table 1) [11]. That the emission derives from the Os(II) site in each case is obvious from comparison of the emission properties with those of $[Os(bipy)_3]^{2+}$, whose emission is at much lower energy than that of $[Ru(bipy)_3]^{2+}$-type chromophores and also has lower intensity and a shorter lifetime. This implies that both complexes show quantitative energy transfer from the Ru(II) chromophore to the Os(II) chromophore, and this is confirmed by the observation that the excitation spectrum matches the absorption spectrum in both cases. This is

quite predictable behaviour: the MLCT excited-state energy of $[Os(bipy)_3]^{2+}$ is lower in energy than that of $[Ru(bipy)_3]^{2+}$ by 2800 cm^{-1}, and the Ru → Os direction for energy transfer is exergonic in both dinuclear complexes irrespective of which metal ion is in which binding site. The fact that no residual Ru-based emission could be detected means that the energy-transfer rate is fast compared to the limits of the apparatus used, i.e. $k_{en} > 5 \times 10^8$ s^{-1}. In fact very many dinuclear complexes are known which exhibit Ru → Os photoinduced energy transfer in this way, and many such Ru(II)/Os(II) diads with differing bridging ligands have been used to compare the efficiencies of different linking units to mediate photoinduced energy transfer [4,13]. In Ru–AB–Os and Os–AB–Ru we can again see the effects of the inequivalence of the two binding sites of the bridging ligand, with the Os-based emission from site B being about 850 cm^{-1} higher in energy than that from site A.

The pair Ru–AB–Re and Re–AB–Ru show a much more fundamental difference in their photophysical properties than do the two Ru–Os complexes, because — as mentioned earlier — the electronic effects arising from the inequivalence of the two binding sites are now comparable to the inherent differences between the properties of the two chromophores [12]. For Ru–AB–Re the room-temperature emission (at all excitation wavelengths) is Ru-based, as shown by the characteristically high intensity and long lifetime compared to the emission from Re-based chromophores, and again the excitation spectrum matches the absorption spectrum. Thus, Re → Ru energy transfer is occurring such that any excitation of the Re chromophore results in energy transfer to, and subsequent emission from, the Ru chromophore in site A. This is the expected direction of energy-transfer considering the relative ^{3}MLCT excited-state energies of the parent $[Ru(bipy)_3]^{2+}$ and $[Re(bipy)(CO)_3Cl]$ chromophores, and Re → Ru energy transfer is known in other dinuclear complexes based on symmetrical bis-bipyridyl bridging ligands [14].

For Re–AB–Ru in contrast, the emission in solution at 298 K is Re-based at all excitation wavelengths. On changing from Ru–AB–Re to Re–AB–Ru, the ^{3}MLCT excited-state energy of the Ru chromophore will rise and that of the Re chromophore will drop (cf. the electrochemical results), such that the lowest excited state is Re-based and Ru → Re now appears to be the favoured direction for energy transfer. At 77 K however the emission from Re–AB–Ru reverts to being Ru-based. This is because the Re-centred MLCT excited state is destabilised by freezing the solvent (which prevents solvent reorganisation following the charge-transfer) *more* than is the Ru-centred MLCT excited state. The lowest-energy MLCT excited state is now Ru-centred [12].

Thus, this pair of complexes shows two interesting features in their energy-transfer characteristics. The first is that swapping the metal fragments between the binding sites, from Ru–AB–Re to Re–AB–Ru, results in a change in the site of emission from Ru-based to Re-based, as described above. The second is that simply cooling Re–AB–Ru from 298 to 77 K results in the site of emission swapping from Re-based back to Ru-based.

2.4. Time-resolved infrared spectroscopy of Ru–AB–Re and Re–AB–Ru

A study of the excited states of Ru–AB–Re and Re–AB–Ru by picosecond time-resolved infra-red (TRIR) spectroscopy provided additional clarification of the energy transfer processes in these two complexes, as this method allows observation and detection of excited states which are not emissive and which therefore cannot be detected by luminescence-based methods [15]. The experiments involved measuring the shift in the carbonyl stretching frequencies of the {Re(bipy)$(CO)_3$Cl} chromophore immediately after laser excitation. Formation of the MLCT excited state of Ru–AB–Re results in a shift of all of the CO stretching vibrations to lower energy by ca. 10 cm^{-1}. This implies formation of a Ru-based MLCT excited state in which an electron is promoted from the Ru[d(π)] orbitals onto the bridging AB ligand. The reduced bridging ligand will in turn make the Re centre more electron-rich, such that back-bonding into the π^* orbitals of the carbonyl ligands will increase and the CO bonds will weaken. The TRIR study therefore is exactly in agreement with the luminescence measurements which also showed the emissive excited state to be Ru-based [12].

For Re–AB–Ru the TRIR spectrum 100 ps after excitation showed a more complicated situation: the CO stretching vibrations of the ground state split into *two* sets of CO vibrations in the excited state, one slightly lower (ca. 10 cm^{-1}) in energy and one much higher (ca. 60 cm^{-1}) in energy [15]. This is only consistent with the presence of two excited states, sufficiently similar in energy that both are significantly populated at 298 K, with equilibration between them being slow on the IR timescale. The set of CO vibrations at slightly lower energy than the ground state is consistent with the presence of a Ru-based MLCT excited state, as described earlier. The set of vibrations at much higher energy than the ground state is in contrast consistent with the presence of a Re-based MLCT excited state, in which an electron is promoted from the Re(I) centre onto the bridging ligand, to give $Re^{II}(AB^{\bullet -})$. The back-bonding to the carbonyl π^* orbitals will be substantially decreased and accordingly their stretching vibrations will become higher in energy. If both states are populated, as the TRIR results suggest, we need to ask why only emission from the Re-based excited state was observed in the luminescence studies. The answer lies in the intrinsically much faster non-radiative decay of the $Re^{II}(AB^{\bullet -})$ excited state (Table 1). The equilibrium distribution of excited-state populations is therefore pulled in one direction towards that state (Re-based) which deactivates most quickly (Fig. 3). This illustrates the power of TRIR spectroscopy as an adjunct to luminescence studies: luminescence spectroscopy alone could not detect the presence of the populated Ru-based MLCT excited state because it is non-emissive in this situation. In Re–AB–Ru it appears that the inherent energy difference between the excited states of $[Ru(bipy)_3]^{2+}$ and [Re(bipy)$(CO)_3$Cl] is almost exactly compensated for by the inequivalence of the two binding sites of the bridging ligand, which renders the two excited states approximately equivalent in energy. The equilibrium between the two excited states can be considered as either an intramolecular energy-transfer between the two MLCT excited states, or (since the bridging ligand is reduced in both cases) as an electron transfer between the two metal centres, i.e. electronic delocalisation.

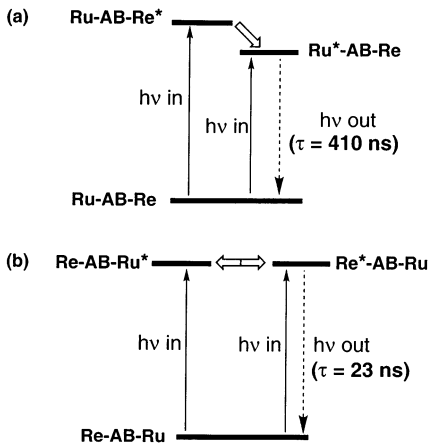

Fig. 3. Luminescence from (a) Ru–AB–Ru and (b) Re–AB–Ru. In case (a) the Ru chromophore is lower in energy, and is the site of emission following either direct excitation or Re → Ru energy-transfer (denoted by the thick arrow). In case (b) the Re and Ru excited-states are almost isoenergetic and in thermal equilibrium (shown by the double-headed arrow); however emission is only seen from the Re chromophore due to its inherently much faster deactivation rate.

3. Non-covalently-linked chromophores: complexes with hydrogen-bonding substituents

3.1. Syntheses of ligands and complexes

In contrast to the work described above based on covalently-linked chromophores, we have also investigated an alternative approach in which mononuclear complexes are functionalised at the periphery with hydrogen-bonding units. This allows two complexes, e.g. a chromophore and a quencher, to be assembled into a single unit by spontaneous association in solution of a complementary pair of pendant hydrogen-bonding groups. The most obvious such groups are the nucleotide bases adenine (A), thymine (T), cytosine (C) and guanine (G), for several reasons. Firstly, complementary hydrogen-bond formation to give the Watson–Crick A/T and C/G base-pairs are very well known, with the C/G triple hydrogen-bond in particular being reasonably strong. Secondly, the free bases are easy to functionalise by alkylation, which allows them to be attached to polypyridyl ligands very easily. Thirdly, the components are commercially available and cheap, in obvious contrast to the many more elaborate artificial hydrogen-bond donor–acceptor units that have been developed for molecular recognition and host–guest chemistry. Others have found these nucleotide bases to be suitable for self-assembly of porphyrin units in solution for similar reasons, and hydrogen-bonded interfaces are known to be able to mediate both photoinduced energy- and electron-transfer between chromophore and quencher units [6].

Attachment of the A, T, C and G units to a bipyridyl ligand via a $–CH_2–$ spacer (Scheme 2) is straightforward, using 5-bromomethyl-2,2′-bipyridine as the alkylat-

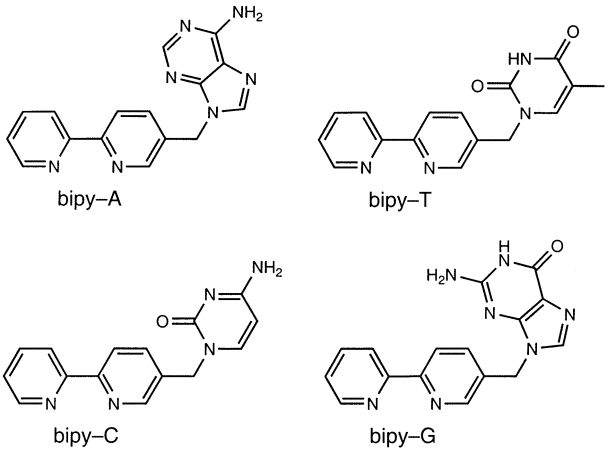

Scheme 2. Structural formulae of the bipyridyl-nucleobase ligands bipy-A, bipy-T, bipy-C and bipy-G.

ing agent [16,17]. The ligands bipy-A, bipy-T and bipy-C could thus be prepared in a one-pot reaction with the preferred regioisomer being obtained in each case (by reaction at N^9 for adenine and N^1 for thymine and cytosine). Only bipy-G requires a more elaborate preparation: direct reaction of guanine with alkyl halides results in alkylation of one of the nitrogen atoms at the hydrogen-bonding site, so the protected derivative 2-amino-6-chloropurine was used to attach to 5-bromomethyl-2,2′-bipyridine by alkylation at the desired position N^9, after which acid hydrolysis produced bipy-G [17]. Reaction of each of these ligands with $[Ru(bipy)_2Cl_2]$ or $[Os(bipy)_2Cl_2]$ as appropriate produced the desired $\{M(bipy)_3\}^{2+}$ complexes (M = Ru, Os) bearing one pendant nucleobase group for hydrogen-bonding. In order to optimise solubility of the complexes in low-polarity solvents, and thereby maximise hydrogen-bonding, 4,4′-^{t}Bu$_2$-bipy was also used as a co-ligand in place of unsubstituted bipy. Electrochemical, spectroscopic and luminescence studies on the complexes show that they retain the basic properties of the $\{M(bipy)_3\}^{2+}$ cores (Table 1), no doubt because the 'insulating' $-CH_2-$ spacer minimises any electronic perturbation of the complex core by the pendant nucleobase.

3.2. Structural studies on metal complexes

Crystal structures of $[Ru(^tBu_2bipy)_2(bipy\text{-}A)][PF_6]_2$ (Fig. 4), $[Os(^tBu_2bipy)_2(bipy\text{-}T)][PF_6]_2$ (Fig. 5) and $[Ru(^tBu_2bipy)_2(bipy\text{-}C)][PF_6]_2$ (Fig. 6) illustrate the hydrogen-bonding abilities of these compounds. $[Ru(^tBu_2bipy)_2(bipy\text{-}A)][PF_6]_2$ (Fig. 4) shows Hoogsteen-type hydrogen-bonding between the pendant adenine units, resulting in formation of a hydrogen-bonded ribbon of adenine moieties running through the crystal. The stronger of the two hydrogen bonds is between the amino group and the adenine N^3 of the adjacent molecule, with the N···N separation being 2.94 Å. The weaker interaction is between the adenine N^1 and one of the hydrogen atoms of the CH_2 fragment of an adjacent molecule, with the N···C separation being 3.52

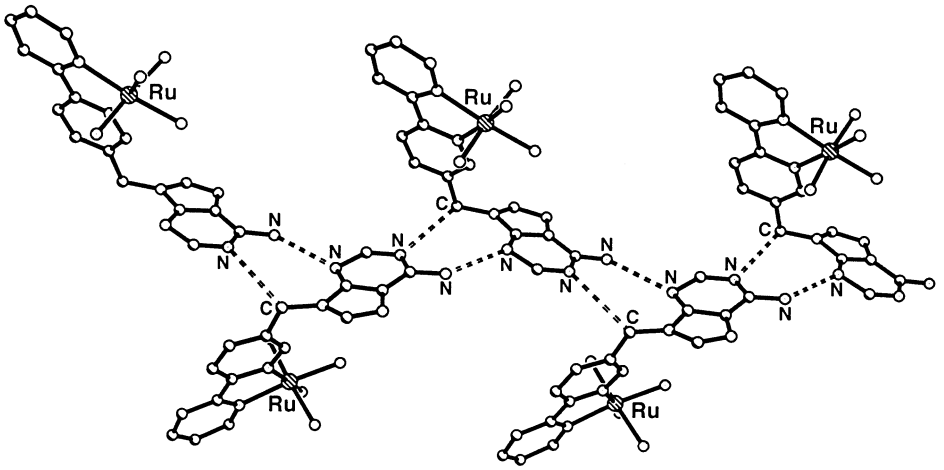

Fig. 4. Crystal structure of $[Ru(^tBu_2bipy)_2(bipy\text{-}A)][PF_6]_2$, showing the ribbon formed by Hoogsteen-type association of the adenine units (the ancillary $^tBu_2$bipy ligands are omitted for clarity).

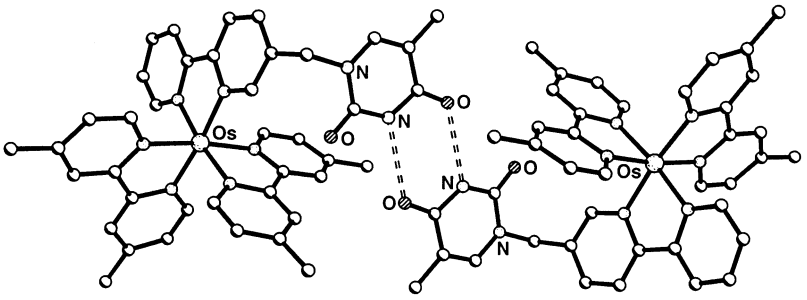

Fig. 5. Crystal structure of $[Os(^tBu_2\text{-}bipy)_2(bipy\text{-}T)][PF_6]_2$, showing the Watson–Crick base-pairing of the thymine units (the disordered ^{t}Bu groups of the $^tBu_2$bipy ligands are omitted for clarity).

Å. It is interesting that the adenine N^7 atom is not involved in hydrogen-bonding, as it is in the structure of 9-methyladenine [18]. However it is likely that a dominant controlling feature in the formation of this hydrogen-bonding ribbon is the requirement to maximise the separation between the positively charged metal complex units, which explains why the $\{Ru(bipy)_3\}^{2+}$ cores are disposed alternately above and below the ribbon.

The crystal structure of $[Os(^tBu_2\text{-}bipy)_2(bipy\text{-}T)][PF_6]_2$ (Fig. 5) shows that two molecules are associated across an inversion centre via a thymine–thymine double N–H···O hydrogen-bond, whose N···O separation of 2.94 Å which lies within the normal range for Watson–Crick hydrogen-bonding. This interaction is similar to that observed in the crystal structure of free thymine (as well as other uracil derivatives), in which the intermolecular N···O distances are 2.81 and 2.84 Å [19]. The slight lengthening of the intermolecular contacts may again be ascribed to electrostatic repulsion between the dicationic complex units.

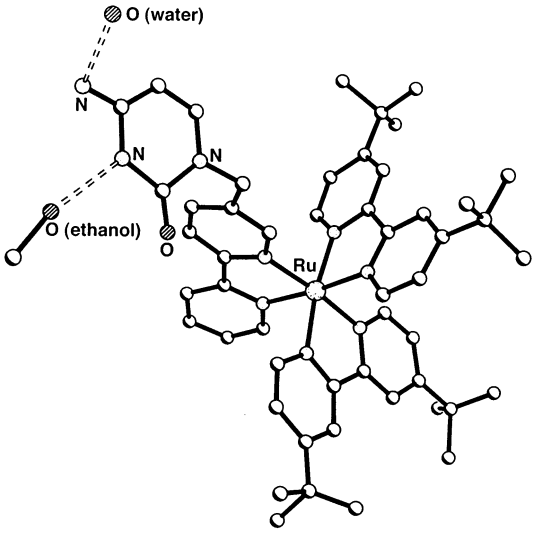

Fig. 6. Crystal structure of $[Ru(^tBu_2\text{-bipy})_2(bipy\text{-}C)][PF_6]_2$, showing association of lattice solvent molecules with the pendant cytosine residue.

In contrast to the above three structures, the crystal structure of $[Ru(^tBu_2\text{-bipy})_2(bipy\text{-}C)][PF_6]_2$ (Fig. 6) shows no self-association between the pendant nucleobase groups, because the cytosine residues are instead involved in hydrogen-bonding interactions with solvent molecules [20]. The heterocyclic N atom is involved in an O–H···N interaction (O···N separation, 2.78 Å) with an ethanol molecule and the amino group is involved in a hydrogen-bonding interaction with a lattice water molecule (O···N separation, 3.08 Å). This nicely illustrates the importance of conducting hydrogen-bonding studies in non-polar solvents, as polar solvents will effectively compete for the hydrogen-bonding sites and prevent the Watson–Crick association in solution.

3.3. Solution studies on hydrogen-bonded Ru···Os associates

Initially we studied the pair $[Ru(^tBu_2bipy)_2(bipy\text{-}A)][PF_6]_2$ (hereafter Ru–A) and $[Os(^tBu_2\text{-bipy})_2(bipy\text{-}T)][PF_6]_2$ (Os–T), which would be expected to associate in solution via a Watson–Crick double hydrogen-bond between the adenine and thymine groups [16]. ^1H NMR titration of a fixed amount of Os–T by adding aliquots of Ru–A showed a steady shift of the thymine N–H proton to lower field. This implies that the equilibrium process of Eq. (1) is fast on the NMR timescale, and standard curve-fitting procedures afforded stability constant values of ca. 120 M^{-1} in CD_2Cl_2 and 60 M^{-1} in CD_3CN, the lower value being obtained in the more polar (competitive) solvent.

$$Ru\text{–}A + Os\text{–}T \rightleftharpoons Ru\text{–}A{:}T\text{–}Os \quad (1)$$

Although association is clearly occurring, at the low concentrations (at most 10^{-4} M) used for solution luminescence studies only ca. 1% of the complex units will be associated, i.e. the equilibrium of Eq. (1) lies almost completely to the left and the properties of the associated Ru–A:T–Os pair cannot be measured in the presence of such an excess of free monomer units.

In contrast the complementary pair $[Ru(^tBu_2bipy)_2(bipy\text{-}C)][PF_6]_2$ (Ru–C) and $[Os(^tBu_2\text{-}bipy)_2(bipy\text{-}G)][PF_6]_2$ (Os–G) can form a much stronger triple hydrogen-bond, and the extent of association between these two in CH_2Cl_2 is such that the associated pair Ru–C:G–Os can be clearly detected in the presence of free monomeric units (Eq. (2)) [17].

$$Ru\text{–}C + Os\text{–}G \rightleftharpoons Ru\text{–}C{:}G\text{–}Os \quad (2)$$

The key experiment is simple: the Ru-based luminescence intensity of an equilibrium mixture of Ru–C and Os–G (each at 10^{-4} M) was measured before and after addition of a few drops of ethanol to the CH_2Cl_2 solution, and it was found to increase by a factor of 1.4 after the ethanol addition. Since addition of ethanol will break the hydrogen-bonding and drive the equilibrium of Eq. (2) to the left-hand extreme, it follows that the gain in Ru-based luminescence occurs because all of the Ru–C is now free and luminescent, whereas originally some of it was quenched by binding in the Ru–C:G–Os associate. From this change in emission intensity we can calculate what fraction of the Ru–C was hydrogen-bonded at this concentration, and hence determine the association constant which is ca. 5000 M^{-1}. Similar results were obtained at several different concentrations of the component parts (Fig. 7) [17].

Thus, in the Ru–C:G–Os associate the Ru-based emission is almost completely quenched, and this quenching is removed when the hydrogen-bond is broken. In a

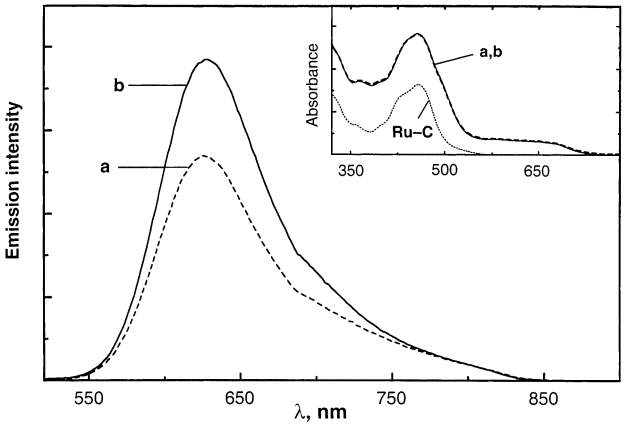

Fig. 7. Luminescence spectra of a CH_2Cl_2 solution of Ru–C and Os–G (both 1.0×10^{-4} M), before (a) and after (b) EtOH addition. The amount of the increase in Ru-centred emission on addition of EtOH, which breaks up the Ru–C:G–Os associate, allows determination of the association constant as ca. 5000 M^{-1}.

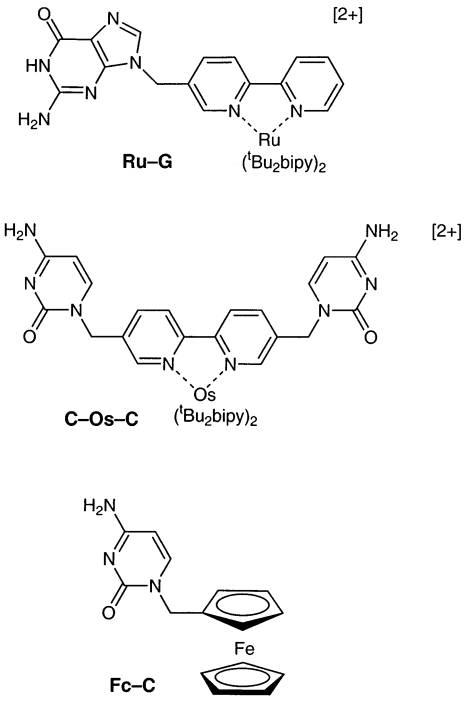

Fig. 8. Structural formulae of Ru–G, C–Os–C and Fc–C.

control experiment (Ru–C with $[Os(^tBu_2bipy)_2(bipy)][PF_6]_2$), no hydrogen-bonding associate can be formed, and addition of EtOH had no effect on the emission properties of the mixture. Time-resolved measurements showed that whereas the free Ru–C had an emission lifetime τ of 350 ns, the bound Ru–C in the Ru–C:G–Os associate in fact had a residual very weak emission with $\tau = 10.5$ ns. From these figures the rate constant for energy-transfer across the hydrogen bond could be determined: based on $k_{en} = 1/\tau_1 - 1/\tau$, the rate constant for this step is $k_{en} = 9.5 \times 10^7\ s^{-1}$ (the average of the values obtained at three different concentrations).

Very similar behaviour was shown by the pair of compounds Ru–G and C–Os–C (Fig. 8), which formed a 1:1 associate Ru–G:C–Os–C in CH_2Cl_2 with $K_{ass} = 1.1 \times 10^4\ M^{-1}$ (we could find no evidence for formation of a trinuclear assembly Ru–G:C–Os–C:G–Ru) [21]. Whereas free Ru–G has an emission lifetime of 450 ns, in the associate Ru–G:C–Os–C the Ru-based emission is nearly completely quenched with a lifetime of 12.5 ns. On this basis the measured Ru → Os intercomponent energy transfer rate constant is $k_{en} = 8.0 \times 10^7\ s^{-1}$. Addition of EtOH breaks the associate, causing virtually complete restoration of the Ru-based luminescence properties (intensity and lifetime) of free Ru–G.

3.4. A Ru···ferrocene hydrogen-bonded assembly

Ferrocene is also known to act as a quencher of $[Ru(bipy)_3]^{2+}$-based emission, although the mechanism is not clear [22]. We therefore investigated the couple Ru–G and Fc–C (where Fc–C is 1-ferrocenylmethylcytosine, Fig. 8) and found that within the Ru–G:C–Fc associate in CH_2Cl_2 there was no significant quenching of the Ru-based luminescence [21]. Although this is a negative result, it has interesting implications. Given the large Ru···Fe separation and the poor overlap between the emission spectra of the energy donor and the absorption spectrum of the acceptor, energy-transfer by the Förster mechanism is not possible. However Ru → Fc energy transfer by a Dexter mechanism (double electron exchange), or Ru ← Fc electron transfer could in principle occur if the bridging pathway allowed a strong enough inter-centre electronic coupling. The absence of any quenching means that the bridging pathway, which includes two saturated methylene groups as well as the C | G interface, results in a very weak electronic coupling which does not support electron-transfer in this case. We can conclude that for Ru–G:C–Os [17] and Ru–G:C–Os–C [21], where efficient energy-transfer across this same interface was observed, energy-transfer is likely to be occurring by the Förster mechanism. This was supported by calculations taking into account the estimated Ru···Os separation and the spectral properties of the two chromophores. Ru → Os photoinduced energy-transfer therefore occurs in Ru–G:C–Os and Ru–G:C–Os–C without any electronic mediation by the H-bonds which only fulfil the purely structural role of holding the Ru and Os centres close together. This may be compared with recent work from other groups which shows that a multiple hydrogen-bond interface can support photoinduced electron-transfer across it [23].

4. Covalently-linked chromophores separated by a macrocyclic spacer

4.1. Syntheses of bis-terpyridyl ligands and structures of complexes

If the pathway through which photoinduced energy- or electron-transfer occurs in a diad complex can be reversibly modified in some way, then there exists the possibility of switching the interaction. One approach to this which we have investigated recently is to use bridging ligands which contain two polypyridyl binding sites separated by a macrocyclic spacer group. Binding of a metal ion by the macrocyclic cavity would cause a substantial electronic, and possibly steric, perturbation; this could be used as the basis for switching the end-to-end photoinduced energy or electron transfer process.

Scheme 3 shows two different bridging ligands which were prepared with this in mind; both are based on a diaza-18-crown-6 (abbreviated hereafter as 'N_2O_4') macrocycle to which the polypyridyl binding sites are linked via functionalisation of the macrocycle N atoms [24]. L^1 is simply prepared by direct reaction of the free diaza-18-crown-6 with 4′-bromo-2,2′:6′,2″-terpyridine in a melt; some of the mono-terpyridyl ligand L^{1a} is also formed. It proved possible by the usual methods to

attach $\{Ru(terpy)\}^{2+}$ and/or $\{Os(terpy)\}^{2+}$ fragments to the termini of L^1 to give dinuclear complexes; however addition of metal ions such as Ba^{2+} showed no significant binding to the N_2O_4 unit. The crystal structure in Fig. 9 shows why.

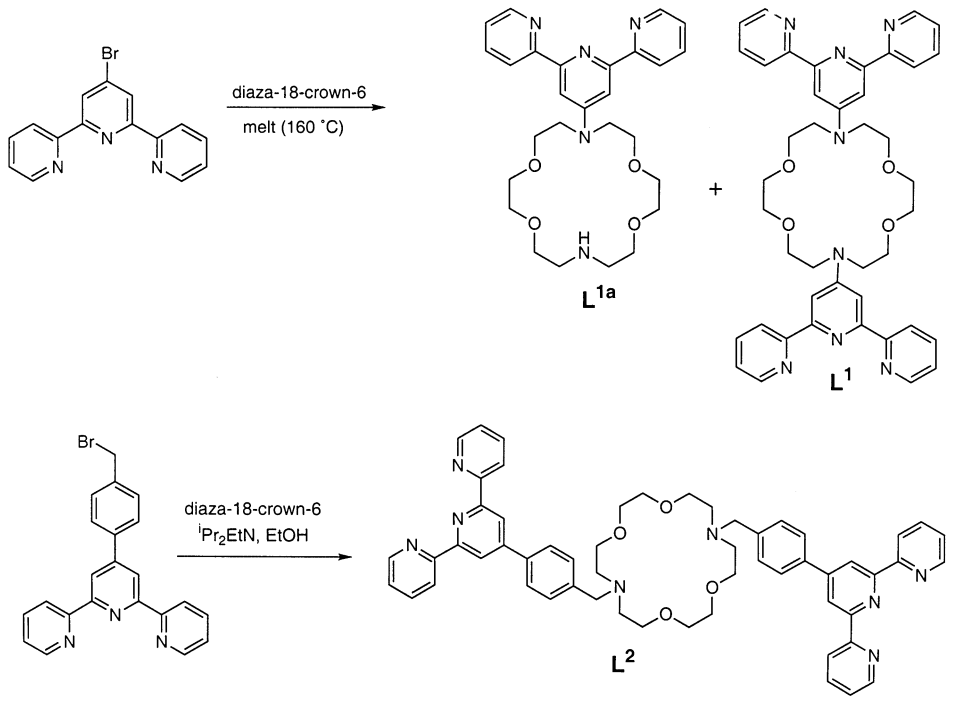

Scheme 3. Syntheses of bis-terpyridyl bridging ligands with macrocyclic spacers between the terpyridyl sites.

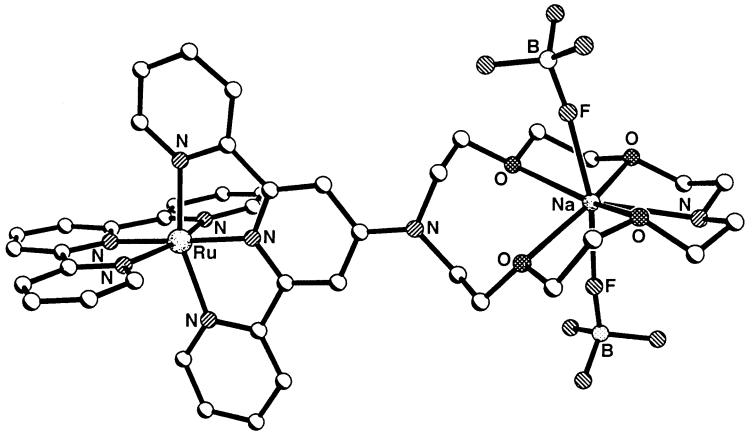

Fig. 9. Crystal structure of the complex cation of $[(terpy)Ru(L^{1a})Na(BF_4)_2][PF_6]\cdot 1.5(acetone)$.

Crystallisation of $[Ru(terpy)(L^{1a})][PF_6]_2$ in the presence of $NaBF_4$ afforded crystals of $[(terpy)Ru(L^{1a})Na(BF_4)_2][PF_6]$ in which the Na^+ ion occupies the N_2O_4 macrocycle, and is also coordinated by two axial $[BF_4]^-$ anions. The important point is that the Na^+ ion is coordinated only by the four oxygen atoms and the free secondary amine site of the macrocycle: the tertiary amine of the macrocycle, which is the site of attachment to the terpyridyl ligand, is not coordinated because its lone pair is in a π-type orbital which is conjugated with the pyridyl ring and therefore delocalised. In the bis-terpyridyl ligand L^1 we therefore expect neither of the (tertiary) amine atoms from the N_2O_4 unit to participate in binding to metal ions, thereby making the macrocycle a very poor ligand.

Use of aliphatic spacers was therefore adopted, as shown by L^2 which is obtained from alkylation of free N_2O_2 with 4′-[(4-bromomethyl)phenyl]-2,2′:6′,2″-terpyridine [24]. The crystal structure of $[\{(terpy)Ru\}_2(\mu\text{–}H_2L^2)][PF_6]_6$ (Fig. 10) illustrates another problem which has now arisen: because the N atoms of the N_2O_4 units are better bases than in L^1, they protonate easily and in this case both amines are protonated giving a 6+ complex. Protonation will of course compete with metal-ion binding so metal-ion binding and photophysical studies will require control of pH.

4.2. Preparation of the bis-bipyridyl ligand L^3 and the diad Ru–Crw–Re

The best photophysical results were obtained with complexes of L^3 [25], which contains bipyridyl rather than terpyridyl metal binding sites; the far superior photophysical properties of the $[Ru(bipy)_3]^{2+}$ unit compared to $[Ru(terpy)_2]^{2+}$ are well known [4]. The complex $[(bipy)_2Ru(\mu\text{-}L^3)Re(CO)_3(H_2O)][PF_6]_3$ (hereafter abbreviated as Ru–Crw–Re) was prepared by the stepwise route outlined in Scheme 4 [25,26], via the mononuclear intermediate $[(bipy)_2Ru(L^3)][PF_6]_2$ which has a pendant bipyridyl site for attachment of the Re fragment.

The crystal structure of the protonated, hydrated form of this mononuclear complex $[Ru(bipy)_2(L^3)][PF_6]_2\cdot HPF_6\cdot H_2O$ (Fig. 11) shows some interesting features. Firstly, the molecule adopts a folded conformation in which the two bipyridyl units attached to the macrocycle lie partially blocking each face. This is a consequence of the arrangement of substituents around the pyramidal N atoms in the macrocycle. Secondly, there is a water molecule held in the centre of the macrocyclic cavity by

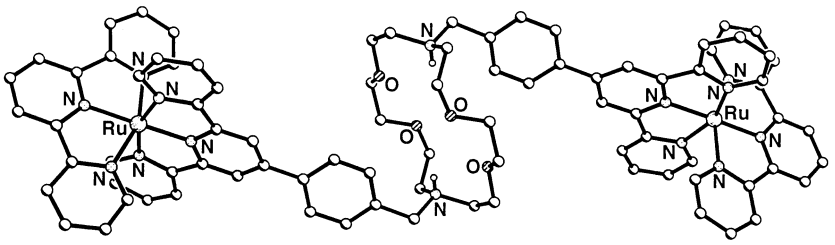

Fig. 10. Crystal structure of the complex cation of $[\{(terpy)Ru\}_2(\mu\text{–}H_2L^2)][PF_6]_6\cdot 2(MeCN)$.

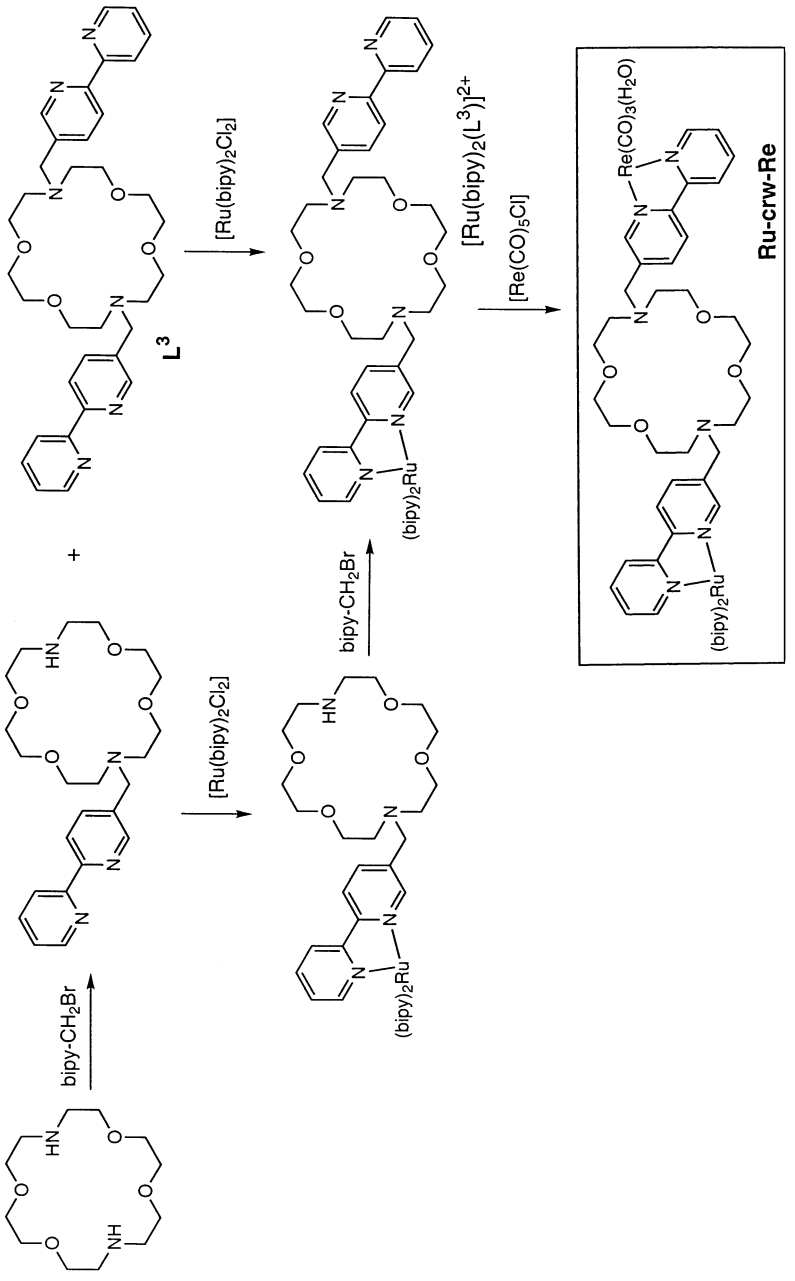

Scheme 4. Synthetic routes to $[(bipy)_2Ru(\mu\text{-}L^3)Re(CO)_3(H_2O)][PF_6]_3$ (Ru–Crw–Re).

three hydrogen-bonding interactions; the relevant distances are O(1)···O(414), 2.87 Å; O(1)···O(426), 2.91 Å; O(1)···N(420), 2.79 Å. The first two of these are consistent with short, strong O–H···O bonds which can be accounted for by the two hydrogen atoms of the water molecule interacting with the ether oxygen atoms of the macrocycle. The N···O separation of 2.79 Å is also indicative of a strong hydrogen bond, which must be of the form N–H···O with the water molecule acting as the acceptor and a protonated nitrogen acting as the donor: this is consistent with the observation of three hexafluorophosphate anions for the Ru^{2+} complex.

Reaction of this complex with $[Re(CO)_5Cl]$ afforded initially the expected complex $[(bipy)_2Ru(\mu\text{-}L^3)Re(CO)_3Cl][PF_6]_2$, but the chloride ligand attached to the Re centre proved to be unexpectedly labile and was replaced by water during chromatographic workup to give $[(bipy)_2Ru(\mu\text{-}L^3)Re(CO)_3(H_2O)][PF_6]_3$ (Ru–Crw–Re). This may be related to the presence of a water molecule held close to the site of ligand substitution by the N_2O_4 macrocycle — an interesting example of supramolecular catalysis [25].

4.3. Photophysical properties of Ru–Crw–Re

The complex Ru–Crw–Re contains $\{Ru(bipy)_3\}^{2+}$ and $\{Re(bipy)(CO)_3(H_2O)\}^{+}$ luminophores, and a macrocyclic spacer (crw) which can fulfil two functions: (i) it can bind a metal ion; (ii) it can act as an electron-donor quencher via the amine nitrogen atom. The photophysical properties of Ru–Crw–Re show four distinct types of behaviour, according to temperature (room temperature or 77 K) and the presence or absence of Ba^{2+} in the macrocycle, as follows. These results are summarised in Table 2 and Scheme 5.

4.3.1. Case (a): room temperature, Ba^{2+} absent

In fluid solvent, only Ru-based luminescence is detected. No emission from the Re-based chromophore occurs because it is quenched by electron transfer from an N atom of the azacrown unit, which is exergonic. That this quenching does *not*

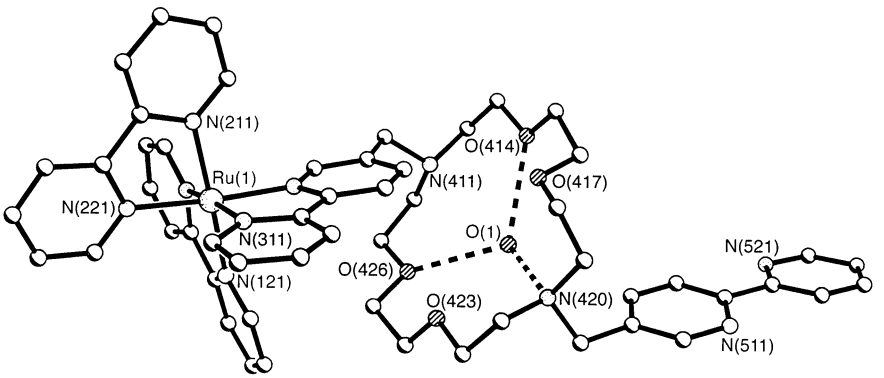

Fig. 11. Crystal structure of the complex cation of $[Ru(bipy)_2(L^3)][PF_6]_2{\cdot}HPF_6{\cdot}H_2O$.

Table 2
Luminescence properties of Ru–Crw–Re and its Ba^{2+} adduct [a]

	295 K			77 K	
	λ_{max} (nm) [b]	$10^2\Phi$ [b]	τ (ns)	λ_{max} (nm) [b]	τ (μs)
Ru–Crw–Re	608	2.8	0.08, [c] 170 [d]	586	0.005, [c] 5.0 [d]
Ru–Crw(Ba)–Re	530, [e] 612 [d]	1.2, [e] 3.6 [d]	62, [e] 195 [d]	500, [e] 588 [d]	0.14, [e] 6.0 [d]
$[Re(AB)(CO)_3Cl]$ [f]	616	1.5	22	535	3.2

[a] Air-equilibrated acetonitrile solvent.
[b] $\lambda_{exc} = 380$ nm (for Ru–Crw–Re and its Ba^{2+} associate, Ru- and Re-based absorption occurs in a ~3:1 ratio).
[c] Very weak residual Re-based emission observed at 520 nm.
[d] Ru-based emission.
[e] Re-based emission.
[f] Included for comparison purposes (see Table 1). Solvent was DMF–CH_2Cl_2 (9:1).

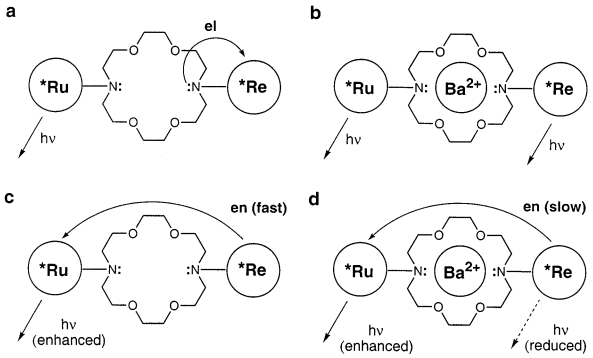

Scheme 5. Principal photophysical processes in Ru–Crw–Re under four different sets of conditions: (a) room temperature, no Ba^{2+}; (b) room temperature, with Ba^{2+}; (c) 77 K, no Ba^{2+}; (d) 77 K, with Ba^{2+}.

arise from Re → Ru energy-transfer (although this would also be thermodynamically favourable) is shown by the observations that (i) selective excitation of the Re fragment does not result in sensitised emission from the Ru centre; and (ii) excitation spectra for the Ru fragment do not show absorbing features from the Re-based chromophore. The chromophores behave essentially independently, with the Re-based chromophore being quenched by electron-transfer from an nearby amine group. Electron-transfer quenching of the Ru-based chromophore in this way would be endergonic and so does not occur.

4.3.2. Case (b): room temperature, Ba^{2+} hosted within crw

Addition of Ba^{2+} to the solution at room temperature, resulting in formation of the Ru–Crw(Ba)–Re associate, inhibits $Re^{II} \leftarrow N_{crw}$ electron transfer because the N lone pair of the N_2O_4 unit is now coordinated to Ba^{2+}. The result is that as more

Ba^{2+} is added, emission from the Re centre becomes 'switched on' resulting in dual luminescence as both Re-based and Ru-based chromophores luminesce independently, at ca. 530 and 610 nm, respectively (Fig. 12). From a plot of Re-based emission intensity versus amount of Ba^{2+} added it is possible to estimate an association constant for Ba^{2+} binding of ca. 5×10^4 M^{-1}, which is rather weak (cf. $K > 10^6$ M^{-1} for Ba^{2+} binding to simple N_2O_4 macrocycles [27]) presumably because of the unfavourable electrostatic effects of attaching Ba^{2+} to a complex which has a charge of $+3$ to start with. Note that $Re \rightarrow Ru$ energy-transfer again does not occur: given the distance involved and the saturated nature of the pathway, $Re \rightarrow Ru$ energy-transfer is too slow to compete with the intrinsic rapid deactivation of the Re centre [$k_d^{Re} = 1/(62 \times 10^{-9})$ s^{-1}] which therefore displays normal luminescence.

4.3.3. Case (c): 77 K, Ba^{2+} absent

In frozen solvent, the charge-separated excited state $N^+\cdots(bipy^{\bullet -})Re^I$ which would arise from the $Re^{II} \leftarrow N_{crw}$ electron-transfer quenching of the Re-based excited state is expected to be destabilized by at least 0.5 eV with respect to what happens in fluid solvent, because repolarisation of the solvent to accommodate the altered charge distribution is no longer possible [28]. This electron-transfer quenching of the Re-based excited state is now endergonic and therefore is switched off. This would have the effect of restoring Re-based emission, apart from the fact that $Re \rightarrow Ru$ energy-transfer can now occur instead, because of the much increased lifetime (μs timescale) of the Re-based excited state at 77 K. The result of this is that electron-transfer quenching of the Re fragment is replaced by $Re \rightarrow Ru$ energy-transfer, such that excitation of the Re component results in sensitised emission from the Ru centre. The residual, weak Re-based luminescence with $\tau_q^{Re,77}$

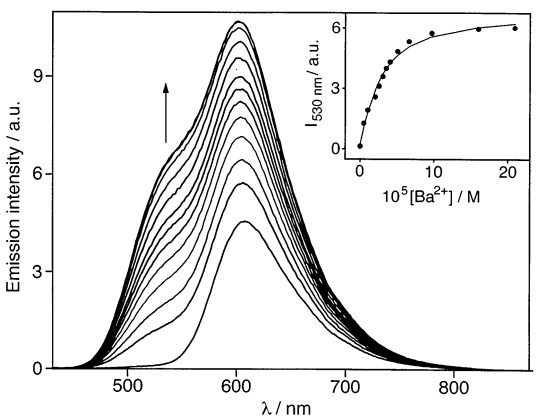

Fig. 12. Changes of the luminescence spectrum of a 2×10^{-5} M acetonitrile solution of Ru–Crw–Re during Ba^{2+} addition; $\lambda_{exc} = 323$ nm. The growth of the Re-based emission band at 530 nm is clear. Inset: fitting of the luminescence intensity measured at 530 nm vs. Ba^{2+} concentration (to determine the association constant).

K = 5 ns allows us to conclude that $k_{en}^{77\ K} \approx 1/\tau_q^{Re,77\ K} = 2.0 \times 10^8\ s^{-1}$ for the energy-transfer rate.

4.3.4. Case (d): 77 K, Ba^{2+} hosted within crw

Again, electron transfer quenching of the Re-based excited state is prevented by the frozen state of the solvent, whereas Re → Ru energy transfer remains energetically allowed and does take place. However compared to case (c) above (in the absence of Ba^{2+}), a substantial increase in the Re-based lifetime is observed, from 5 ns in the absence of Ba^{2+} to 140 ns in the presence of Ba^{2+}. Since the near-complete quenching of Re-based emission in the absence of Ba^{2+} could be ascribed to Re → Ru energy transfer, the partial restoration of the Re-based emission in the presence of Ba^{2+} is indicative of a slower Re → Ru energy transfer step, with $k_{en}^{77\ K,Ba} \approx 1/\tau_q^{Re,77\ K,Ba} = 1/(140\ ns) = 7 \times 10^6\ s^{-1}$. Comparison with the value of $k_{en}^{77\ K} = 2.0 \times 10^8\ s^{-1}$ in the absence of Ba^{2+} (case (c)) shows that incorporation of Ba^{2+} into the macrocycle of Ru–Crw–Re at 77 K slows down the Re → Ru energy transfer process by about a factor of 30.

The most likely explanation for this is that binding of Ba^{2+} in the azacrown moiety results in a conformational rearrangement such that the Ru and Re centres move further apart. The Ru centre has a 2+ charge and the Re centre is 1+; it is reasonable that a dication in the macrocycle should repel them both, giving a greater Ru···Re separation, on electrostatic grounds. Although coordination of Ba^{2+} might also be expected to have an electronic effect on the bridging pathway, the entirely saturated nature of the bridging group means that it is unlikely to participate in long-range electron-transfer processes such as Dexter energy-transfer, and that it is the metal–metal separation (determined by conformational effects) which are more significant in controlling the energy-transfer rate.

Thus, in Ru–Crw–Re a variety of inter-component electron- and energy-transfer quenching processes can occur, which are both modulated by the presence or absence of Ba^{2+} in the central macrocycle as well as by cooling from room temperature to 77 K. The 30-fold alteration in the rate of photoinduced Re → Ru energy transfer at 77 K, arising from a metal-ion induced conformational change, is particularly interesting from the point of view of developing switchable photochemical devices.

5. Covalently-linked chromophores separated by a poly(oxy-ethylene) spacer

Following our observation of how the rate of photoinduced energy-transfer between metal components can be altered by a conformational change in the complex (Section 4.3) we were interested to investigate a bridging ligand with a greater degree of conformational flexibility. For this we chose a poly(oxyethylene) chain derived form pentaethyleneglycol linking two bipyridyl units to give L^4 (Scheme 6) [29]. Both polyethylene glycol [30] and simple model compounds such as dimethoxyethane [31] have strongly solvent-dependent conformations. In these molecules the conformation about the central C–C bond of the OCH_2CH_2O unit is

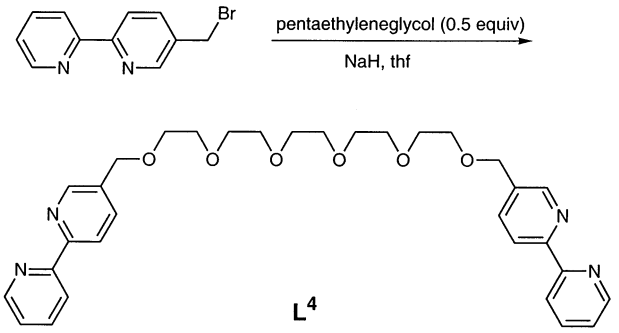

Scheme 6. Synthesis of L^4.

predominantly *trans* in a low-polarity medium, but predominantly *gauche* in a high-polarity medium. The *gauche* conformation, which results in a higher dipole moment for the poly(oxoethylene)chain, is also associated with a more expanded structure such that the end-to-end distance is greater in a higher-polarity solvent.

Successive attachment of $\{Ru(bipy)_2\}^{2+}$ and $\{Os(bipy)_2\}^{2+}$ fragments to the termini of L^4 afforded $[(bipy)_2Ru(\mu\text{-}L^4)Os(bipy)_2][PF_6]_4$, (abbreviated Ru-$L^4$-Os) in which the separation between the Ru and Os components will depend on the conformation of the poly(oxyethylene) chain, which in turn is dependent on the solvent polarity. Fig. 13 shows the luminescence spectra obtained by exciting samples of Ru–L^4–Os in mixed CH_3OH–CH_2Cl_2 solvent of varying proportions. The excitation wavelength was 450 nm so that both the Ru-based and Os-based chromophores were both excited, in a fixed ratio of approximately 1:0.8. The luminescence spectra feature two band maxima, at ca. 600 nm (Ru-based emission)

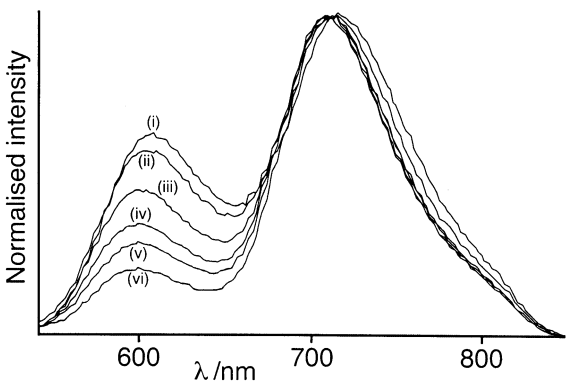

Fig. 13. Normalised luminescence spectra of Ru-L^4-Os in mixed MeOH–CH_2Cl_2 solvents (spectroscopic grade) of proportions (MeOH:CH_2Cl_2): (i) 100:0; (ii) 80:20; (iii) 60:40; (iv) 40:60; (v) 20:80; (vi) 0:100. The solutions were isoabsorptive at the excitation wavelength (450 nm) and the spectra are normalised to the Os-based emission.

and ca. 710 nm (Os-based emission). The relatively low intensity of the Ru-based emission compared to that of the mononuclear model complex $[Ru(bipy)_2L^4][PF_6]_2$ ($Ru–L^4$) is consistent with the occurrence of ca. 90% quenching of the Ru-based emission, due to $Ru \rightarrow Os$ energy transfer ($\Delta G - 0.3$ eV). Thus, the band at around 600 nm is due to a residual (ca. 10%) Ru-based emission, and the band at around 710 nm band is Os-based, with a luminescence intensity which includes contributions from both direct excitation (from 450 nm irradiation) and additional sensitisation following $Ru \rightarrow Os$ energy transfer. It can be seen that as the solvent polarity decreases (from pure MeOH to pure CH_2Cl_2), the Ru-based emission steadily decreases in intensity with respect to the Os-based emission, consistent with improved $Ru \rightarrow Os$ energy transfer arising from a shorter metal–metal separation.

This was confirmed by analysis of the time-resolved luminescence decay of $Ru–L^4–Os$, which was measured in the same mixed-solvent system at the wavelengths of the two emission band maxima. At 600 nm a single (Ru-based) exponential decay was found; at 710 nm the Os-based decay took place according to a dual exponential law, with a rise time and a decay time. We found that in each case the Ru-based decay time (obtained at 600 nm) corresponds to the Os-based rise time (observed at 710 nm), exactly consistent with the occurrence of $Ru \rightarrow Os$ energy transfer. Also, on the basis of $k_{en} = 1/\tau_q - 1/\tau$ we could obtain the $Ru \rightarrow Os$ energy transfer rate constant as a function of solvent composition (where τ is the lifetime of the reference complex, $Ru–L^4$). The results are shown graphically in Fig. 14. It is clear that improved quenching of the Ru emission as the solvent polarity decreases is accompanied by improved $Ru \rightarrow Os$ energy transfer arising from a shorter metal–metal distance.

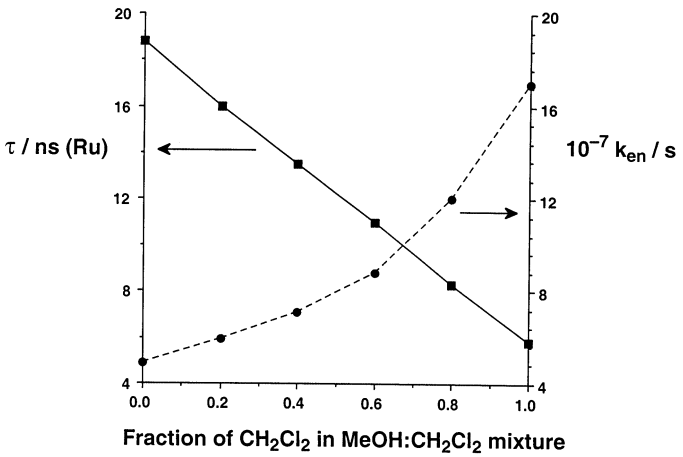

Fig. 14. Photophysical behaviour of $Ru–L^4–Os$ in mixed $MeOH–CH_2Cl_2$ solvents, showing the steady decrease of Ru-based emission lifetime (squares, solid line) and the concomitant increase in $Ru \rightarrow Os$ energy-transfer rate constant (circles, dashed line) as solvent polarity decreases.

Assuming that the Ru→Os energy transfer in this complex arises from the through-space dipole–dipole (Förster) mechanism, which seems reasonable in view of the absence of a conjugated pathway which would be required for the double electron exchange (Dexter) mechanism, it is possible to estimate the metal–metal separation from Eq. (3).

$$k_{en}^{F} = \frac{8.8 \times 10^{-25} K^2 \Phi}{d_{MM}^6 n^4 \tau} J^F \quad (3)$$

In this equation Φ and τ are the luminescence quantum yield and lifetime, respectively, of the energy donor (Ru–L^4); J^F is the integral overlap between the luminescence spectrum of the donor (Ru chromophore) and the absorption spectrum of the acceptor (Os chromophore), K^2 is a geometric factor (taken as 2/3), and n is the refractive index of the solvent. From Eq. (1) and by using the pertinent spectroscopic and calculated parameters ($J^F = 4.7 \times 10^{-14}$ cm^6 mol^{-1} in both solvents), we conclude that $d_{MM} = 15$ and 12 Å in neat CH_3OH and CH_2Cl_2, respectively. These values may be compared with the calculated end-to-end distance of 22 Å for the fully extended ligand L^4 [29].

This observation is interesting for a variety of reasons. With longer poly(oxoethylene) bridging units it will be possible to use the extent of Ru→Os energy transfer as a direct measure of the oligomer conformation in solution. In addition, metal–metal separations may be derived from alternative methods such as small-angle X-ray scattering which will provide a useful comparison with the distances derived from luminescence studies. By substituting electron-accepting quenchers (e.g. diquat) for the energy-accepting $[Os(bipy)_3]^{2+}$ unit, long-range photoinduced electron-transfer in flexible chromophore–quencher systems will also be amenable to study.

6. Conclusions

The four separate systems described above illustrate different aspects of the control of photoinduced energy-transfer in diad assemblies, which is a persistent theme of our work. In the quaterpyridine complexes, the direction of energy-transfer (Re→Ru or Ru→Re) may be altered by exploiting the electronic inequivalence of the two bipyridyl binding sites. The hydrogen-bonded complexes show how assemblies of interacting components can be prepared reversibly from simple mononuclear building blocks without the need for using covalent bonds to link the components together irreversibly. The final two systems, with macrocyclic or poly(oxyethylene) spacers, show how control of the conformation of a flexible molecule — and hence the separation between the interacting units — can be achieved by external perturbations such as metal-ion binding or altering the solvent composition. These offer interesting possibilities for the development of new molecular assemblies with switchable photophysical behaviour.

Acknowledgements

It is a pleasure to acknowledge the efforts of all of our collaborators and the members of the research groups in Bristol and Bologna who between them have made this work possible; their names appear in the references below. Financial support has been provided by EPSRC (UK), the CNR (Italy), and the EU COST programme (action D11).

References

[1] V. Balzani, F. Scandola, Supramolecular Photochemistry, Ellis Horwood, Chichester, UK, 1991.
[2] H. Kurreck, M. Huber, Angew. Chem., Int. Ed. Engl. 34 (1995) 849.
[3] M.R. Wasielewski, Chem. Rev. 92 (1992) 435.
[4] (a) J.-P. Sauvage, J.-P. Collin, J.-C. Chambron, S. Guillerez, C. Coudret, V. Balzani, F. Barigelletti, L. De Cola, L. Flamigni, Chem. Rev. 94 (1994) 993. (b) F. Barigelletti, L. Flamigni, Chem. Soc. Rev. 29 (2000) 1.
[5] V. Balzani, A. Juris, M. Venturi, S. Campagna, S. Serroni, Chem. Rev. 96 (1996) 759.
[6] M.D. Ward, Chem. Soc. Rev. 26 (1997) 365.
[7] M.D. Ward, J. Chem. Soc., Dalton Trans. (1993) 1321. Note that in this paper the ligand was incorrectly assumed to be 2,2′:4′,2″:6″,2‴-quaterpyridine, arising from a C^6/C^4 coupling of two bpy radical anions, on the basis of the ^1H NMR spectrum (14 inequivalent protons) and the tendency of pyridine [9] and other bipyridines [10] to couple solely at the C^6 and C^4 positions under the same conditions.
[8] R.L. Cleary, D.A. Bardwell, M. Murray, J.C. Jeffery, M.D. Ward, J. Chem. Soc., Perkin Trans. 2 (1997) 2179.
[9] G.R. Newkome, D.C. Hager, J. Org. Chem. 47 (1982) 599.
[10] T. Kaufmann, R. Otter, Chem. Ber. 116 (1983) 479.
[11] V. Balzani, D.A. Bardwell, F. Barigelletti, R.L. Cleary, M. Guardigli, J.C. Jeffery, T. Sovrani, M.D. Ward, J. Chem. Soc., Dalton Trans. (1995) 3601.
[12] D.A. Bardwell, F. Barigelletti, R.L. Cleary, L. Flamigni, M. Guardigli, J.C. Jeffery, M.D. Ward, Inorg. Chem. 34 (1995) 2438.
[13] (a) A. Harriman, R. Ziessel, Chem. Commun. (1996) 1707. (b) L. De Cola, P. Belser, Coord. Chem. Rev. 177 (1998) 301.
[14] (a) S. Van Wallandael, M.W. Perkovic, D.P. Rillema, Inorg. Chim. Acta 213 (1993) 253. (b) S. Van Wallandael, D.P. Rillema, Coord. Chem. Rev. 111 (1991) 297. (c) M. Furue, M. Naiki, Y. Kanematsu, T. Kushida, M. Kamachi, Coord. Chem. Rev. 111 (1991) 221.
[15] J.R. Schoonover, A.P. Shreve, R.B. Dyer, R.L. Cleary, M.D. Ward, C.A. Bignozzi, Inorg. Chem. 37 (1998) 2598.
[16] C.M. White, M.F. Gonzalez, D.A. Bardwell, L.H. Rees, J.C. Jeffery, M.D. Ward, N. Armaroli, G. Calogero, F. Barigelletti, J. Chem. Soc., Dalton Trans. (1997) 727.
[17] N. Armaroli, F. Barigelletti, G. Calogero, L. Flamigni, C.M. White, M.D. Ward, Chem. Commun. (1997) 2181.
[18] T.J. Kistenmacher, M. Rossi, Acta Crystallogr., Sect. B 33 (1977) 253.
[19] K. Ozeki, N. Sakabe, J. Tanaka, Acta Crystallogr., Sect. B 25 (1969) 1038.
[20] C.M. White, K.L.V. Mann, J.C. Jeffery, M.D. Ward, unpublished results.
[21] S. Encinas, N.R.M. Simpson, P. Andrews, M.D. Ward, C.M. White, N. Armaroli, F. Barigelletti, A. Houlton, New J. Chem. 24 (2000) 987.
[22] E.J. Lee, M.S. Wrighton, J. Am. Chem. Soc. 113 (1991) 8262.
[23] T.H. Ghaddar, E.W. Castner, S.S. Isied, J. Am. Chem. Soc. 122 (2000) 1233.
[24] B. Whittle, S.R. Batten, J.C. Jeffery, L.H. Rees, M.D. Ward, J. Chem. Soc., Dalton Trans. (1996) 4249.

[25] S. Encinas, K.L. Bushell, S.M. Couchman, J.C. Jeffery, M.D. Ward, L. Flamigni, F. Barigelletti, J. Chem. Soc., Dalton Trans. (2000) 1783.
[26] Although L^3 could be obtained in a single step from alkylation of free N_2O_4 with two equivalents of 5-bromomethyl-2,2′-bipyridine, reaction with one equivalent of $[Ru(bipy)_2Cl_2]$ to give the necessary intermediate mononuclear complex $[(bipy)_2Ru(L^3)][PF_6]_2$ was complicated by the fact that the product was contaminated with both free L^3 and the dinuclear complex $[\{(bipy)_2Ru\}_2(\mu\text{-}L^3)][PF_6]_4$. This mixture was not easy to separate, and so the alternative stepwise route of Scheme 4 was used instead which gave excellent yields at every step.
[27] (a) R.M. Izatt, K. Pawlak, J.S. Bradshaw, R.L. Bruening, Chem. Rev. 91 (1991) 1721. (b) R.D. Hancock, A.E. Martell, Chem. Rev. 89 (1989) 1875.
[28] (a) G.L. Gaines III, M.P. O'Neil, W.A. Svec, M.P. Niemckziyk, M.R. Wasielewski, J. Am. Chem. Soc. 113 (1991) 719. (b) I.R. Gould, S. Farid, Acc. Chem. Res. 29 (1996) 522.
[29] N.C. Fletcher, M.D. Ward, S. Encinas, N. Armaroli, L. Flamigni, F. Barigelletti, Chem. Commun. (1999) 2089.
[30] M. Björling, G. Karlström, P. Linse, J. Phys. Chem. 95 (1991) 6706.
[31] M. Andersson, G. Karlström, J. Phys. Chem. 89 (1985) 4957.